**F. Benmebarek[1], L. Alloui[1], Y. Gabi[2], S. M. Mimoune[1], B. Wolter[2]**

Laboratoire de Modélisation des Systèmes Energétiques – LMSE; Département d'Electrotechnique, Université Mohamed Kheider, Biskra, Algeria (1), Fraunhofer Institute for Nondestructive Testing IZFP, Saarbrucken 66123, Germany (2)

doi:10.15199/48.2024.02.25

# Three-Dimensional Numerical Modelling of Eddy Current System Using the Finite Volume Method

***Abstract**. The accurate modeling of ferromagnetic magnetic behavior and implementation of magnetic law into a solving procedure of nonlinear partial differential equations, derived from Maxwell's equations are necessary for the design and simulation of electrical engineering applications.*
*The finite element methods are widely used in literature for solving electromagnetic problems. Partial differential equations are generally nonlinear due to the strong nonlinear character of ferromagnetic materials. However, there are other numerical methods, which can be used for design and can offer better numerical stability, such as, the finite volume method (FVM). In this work, FVM simulation results of computer code developed and implemented under MATLAB environment is detailed. The nondestructive eddy current inspection situation on multilayered material is described in three-dimensional modeling problem. The goal is to present a stable numerical model able to solve a highly non-linear problem requiring a very fine mesh with various magnetic properties from one region to another. The confrontation between the experiments and simulations validate the developed FVM models.*

***Streszczewnie**. Dokładne modelowanie zachowania magnetycznego ferromagnetyku i implementacja prawa magnetycznego do procedury rozwiązywania nieliniowych równań różniczkowych cząstkowych, wyprowadzonych z równań Maxwella, są niezbędne do projektowania i symulacji zastosowań w elektrotechnice. Metody elementów skończonych są szeroko stosowane w literaturze do rozwiązywania problemów elektromagnetycznych. Równania różniczkowe cząstkowe są na ogół nieliniowe ze względu na silną nieliniowość materiałów ferromagnetycznych. Istnieją jednak inne metody numeryczne, które można zastosować w projektowaniu i które mogą zapewnić lepszą stabilność numeryczną, takie jak metoda objętości skończonych (FVM). W pracy szczegółowo opisano wyniki symulacji FVM kodu komputerowego opracowanego i zaimplementowanego w środowisku MATLAB. Nieniszcząca sytuacja kontroli prądów wirowych materiału wielowarstwowego jest opisana w problematyce modelowania trójwymiarowego. Celem jest przedstawienie stabilnego modelu numerycznego zdolnego do rozwiązania wysoce nieliniowego problemu wymagającego bardzo drobnej siatki o różnych właściwościach magnetycznych w zależności od regionu. Konfrontacja eksperymentów i symulacji weryfikuje opracowane modele FVM.* (***Trójwymiarowe modelowanie numeryczne układu prądów wirowych przy użyciu metody objętości skończonych***)

**Keywords:** Three-Dimensional Numerical Modelling, Eddy Current System, Finite Volume Method.
**Słowa kluczowe**: Trójwymiarowe modelowanie numeryczne, układ prądów wirowych, metoda objętości skończonych

## Introduction

Significant improvements in material science have significantly affected their exploitation in engineering applications, especially in highly developed industries. In such application, it is necessary to have reliable measurement techniques that evaluate correctly the properties of the materials. Several measurement techniques are used; such as optical and electron microscopy for microstructure analysis and destructive testing methods for the determination of mechanical targets such as: tensile strength, elongation, hardness, etc [1]. However, due to the cost and production speed, it is necessary to predict the properties in a short time and real time. This can be achieved by non-destructive testing (NDT) which is widely used in the aircraft maintenance, particle accelerators and in metallurgical industry; such coating evaluations and material thickness determination [2].

For the improvement of non-destructive testing and to guarantee better functional dependence between the micro-magnetic measurement quantities and the micro structural characteristics and/or material properties (calibration), many equipment and variants of electromagnetic sensors have been developed [3]. However, the complexity of materials makes calibrate of the NDT techniques limited. To overcome these limitations and correctly predict the magnetic behavior of materials in different situations, several analytical and numerical models have been proposed. The analytical models have the advantage of simplicity in terms of cost and time compared to the numerical models. However, the analytical methods reveal their limits in complex geometries and properties (anisotropy, nonlinear character). Nevertheless, the development of new electromagnetic designs requires precise simulation tools. Under these conditions, numerical simulations are the most favorable and large interest in NDT domain where generally, the FEM is widely used [4-5-6-7].Furthermore, this method is the most popular and the most flexible numerical technique [8-9] to determine the approximated solution of the partial differential equations in engineering [9]. However, there are simpler numerical methods and easier to implement in a computational environment, such as the finite volume method (FVM) [10-11]. This method can correctly deal with strong nonlinear problems. It offers comfortable numerical stability to solve such problems compared to the FEM [10-11]. Beside this, the integral form in the FVM method has more explicitly physical meaning than other numerical methods [6].Furthermore, it offers similar flexibility as FEM method for solving complex media.

The first time where, FVM was introduced into electromagnetic computational problem (CEM) by Shankar et al. [12]. Many works presented in literature focus on solving electromagnetic problems is one-dimensional [13] or even two-dimensional [6-14-15].The models are mainly defined by differential equations, which are based on the conservation principle defined by the divergence law [16]. Nevertheless, the basic formula of the FVM is not adapted for electromagnetic system modeling in the three-dimensional cases [16]. A new scheme of the FVM, makes the 3D problem solving possible. This new approach which is developed in our previous works, has been applied only for the 3D modeling systems of diamagnetic materials where the magnetic permeability does not vary from one environment to another[10-16-17]. In this context, the new approach for the 3Dmodeling system is applied on ferromagnetic materials, with various magnetic properties. For this purpose, a mathematical-numerical model is developed and implemented under Matlab environment. The robustness of the proposed work is evaluated by comparison between simulation and the experimental results.

## Mathematical and Numerical Models

The model consists on a 3D sketch of an eddy current probe head and multi-layered sample. The model is illustrated in Figure 1.The sample is then magnetized via the ferrite yoke, which have three arms with the inner and outer pole distances of 12 mm and 18 mm. The simulation parameters are summarize din Table 1.The gap between yoke and the specimen is set to 1mm. The magnetizing coil is wound around the central arm of the yoke (Figure 1).

Table 1. Simulation and measurement set up

| Setup parameter | Value |
|---|---|
| Low frequency excitation $f_{LF}$ | 50 Hz |
| High frequency excitation $f_{HF}$ | 150 KHz |
| Ferrite Yoke [7] | JA: Ms = 1.4110[6]; α=1.4710[-4], a = 85.73, c = 0.316, k 65.53and σ = 6 MS/m. |
| Magnetization coil | 100 turns/4 mm external diameter |

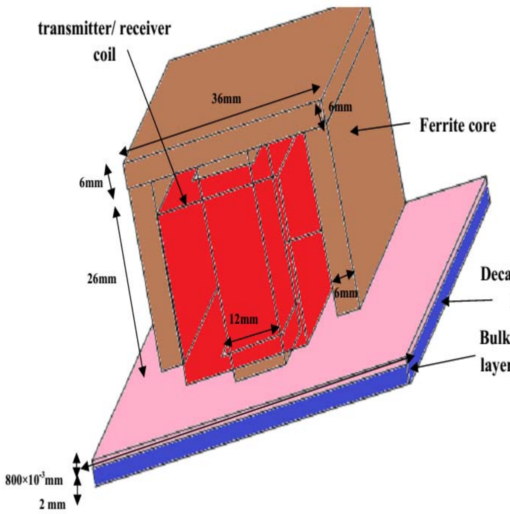


Fig.1. Sketch in 3D.

The layered sample is represented via three layers: decarburized, an intermediate and bulk layer. Two specimen are tested, both have various decarburized layer thickness : 200 μm and 800 μm. A sinusoidal current with frequency ranging from 50 Hz to 150 kHz is applied to the coil for both samples. The measurements are performed on absolute mode. The physical properties and the dimensions of sample layers are given in Table-2.

Table 1. Geometry and physical properties of a sample

| Layer | Thickness | Magnetic permeability μr |
|---|---|---|
| Decarburized | **200 μm** | **250** |
| Intermediate | **600 μm** | **200** |
| Bulk | **2000μm** | **50** |

The electrical resistivity of the different sample layers varies in the range of ρ = [1.49e-7 - 1e-7] Ω.m from the surface to the bulk. The numerical analysis of the studied electromagnetic device is processed by solving the three dimensional (3D) electromagnetic equation obtained from Maxwell's equations. For resolution, it is necessary to add penalty term, which is expressed in following:

$$(1) \quad \nabla \times (\nu \nabla \times \boldsymbol{A}) - \nabla \nu \nabla . \boldsymbol{A} + \sigma \left( \frac{\partial \boldsymbol{A}}{\partial t} + \nabla V \right) = \boldsymbol{J_s}$$

$$(2) \quad \nabla \left( -\sigma \left( \frac{\partial \boldsymbol{A}}{\partial t} + \nabla V \right) \right) = 0$$

In both equations (1) and (2), A and V are respectively the magnetic vector potential and the electric scalar potential. The physical properties υ and σ represent respectively the magnetic reluctivity and the electrical conductivity. The right term of equation (1) Js represents the source current density. The system of partial differential equations (3) and (4) is solved in Cartesian coordinates (x, y, z). The computation of both voltage module and phase are then performed via the resolution of partial differential equations system in terms of magnetic vector potential A and electric scalar potential V formulation.

In the following, only one component of partial differential is represented in equations (1) and (2) along x coordinate. The development is then expressed as following:

$$(3) \quad \begin{aligned} & \frac{\partial}{\partial y}(\upsilon \frac{\partial A_y}{\partial x} - \upsilon \frac{\partial A_x}{\partial y}) - \frac{\partial}{\partial z}(\upsilon \frac{\partial A_x}{\partial z} - \upsilon \frac{\partial A_z}{\partial x}) - \\ & \frac{\partial}{\partial x}(\upsilon \frac{\partial A_x}{\partial x} + \upsilon \frac{\partial A_y}{\partial y} + \upsilon \frac{\partial A_z}{\partial z}) + \\ & \sigma(\frac{A_x}{\partial t} + \frac{\partial V}{\partial x}) = J_{Sx} \end{aligned}$$

$$(4) \quad \begin{aligned} & \frac{\partial}{\partial x}(\sigma(\frac{\partial A_x}{\partial t} + \frac{\partial V}{\partial x}))dv + \\ & \frac{\partial}{\partial y}(\sigma(\frac{\partial A_y}{\partial t} + \frac{\partial V}{\partial y})) + \\ & \frac{\partial}{\partial z}(\sigma(\frac{\partial A_z}{\partial t} + \frac{\partial V}{\partial z})) = 0 \end{aligned}$$

The developments concerning the others coordinates y and z are obtained at the same time but not given here. The finite volume discretization method applied to equations (3) and (4) allow, for each elementary volume (*ve*) of solving domain, to deduce the following equations:

$$(5) \quad \begin{aligned} & \iiint_{ve} \frac{\partial}{\partial y}(\upsilon \frac{\partial A_y}{\partial x} - \upsilon \frac{\partial A_x}{\partial y}) dv - \iiint_{ve} \frac{\partial}{\partial z}(\upsilon \frac{\partial A_x}{\partial z} - \upsilon \frac{\partial A_z}{\partial x}) dv - \\ & \iiint_{ve} \frac{\partial}{\partial x}(\upsilon \frac{\partial A_x}{\partial x} + \upsilon \frac{\partial A_y}{\partial y} + \upsilon \frac{\partial A_z}{\partial z}) dv + \\ & \iiint_{ve} \sigma(\frac{A_x}{\partial t} + \frac{\partial V}{\partial x}) dv = \iiint_{ve} J_{Sx} dv \end{aligned}$$

$$(6) \quad \begin{aligned} & \iiint_{ve} \frac{\partial}{\partial x}(\sigma(\frac{\partial A_x}{\partial t} + \frac{\partial V}{\partial x})) dv + \iiint_{ve} \frac{\partial}{\partial y}(\sigma(\frac{\partial A_y}{\partial t} + \frac{\partial V}{\partial y})) dv + \\ & \iiint_{ve} \frac{\partial}{\partial z}(\sigma(\frac{\partial A_z}{\partial t} + \frac{\partial V}{\partial z})) dv = 0 \end{aligned}$$

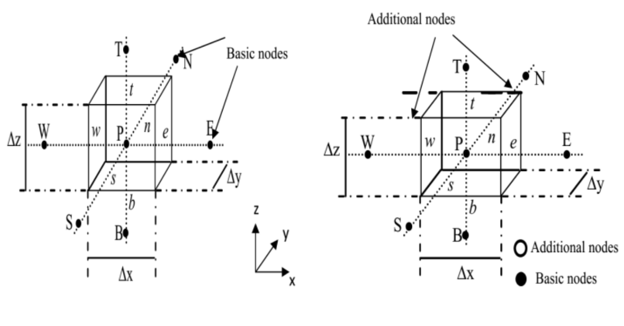


-a- -b-

Fig.1. Elementary volume, a- Classic scheme, b- New scheme

The classic discretization scheme (Figure.2.a.) permits to treat easily the crossed terms (the differential terms such as:

(7) $$\iiint_{ve}\frac{\partial}{\partial i}(\upsilon\frac{\partial A_j}{\partial i})dv\,)$$

with, i and j represent x, y and z coordinates. These terms are similar to those obtained from two-dimensional electromagnetic models or even by three-dimensional models managed by partial differential equations.

The discretization in finite volumes of equation (7) is carried out for each Cartesian coordinate x, y and z in an elementary volume represented in figure 2.a. Thus, for the y-coordinate case, the discretization scheme leads to the following formula:

(8)
$$\iiint_{ve}\frac{\partial}{\partial y}(\upsilon\frac{\partial A_x}{\partial y})dv =$$
$$\int_{wb}^{et}\!\!\int(\upsilon\frac{\partial A_X}{\partial y})\Big|_s^n dxdz = \int_{wb}^{et}\!\!\int\left[(\upsilon\frac{\partial A_X}{\partial y})\Big|_n - (\upsilon\frac{\partial A_X}{\partial y})\Big|_s\right]dxdz$$
$$=\left[(\upsilon\frac{\partial A_X}{\partial y})\Big|_n - (\upsilon\frac{\partial A_X}{\partial y})\Big|_s\right]\Delta x\Delta z =$$
$$\left[\upsilon_n\frac{(A_{XN}-A_{XP})}{\Delta yn} - \upsilon_s\frac{A_{XP}-A_{XS}}{\Delta ys})\right]\Delta x\Delta z$$

In figure (2.a), υn and υs are defined as the magnetic reluctivities at nodes n and s of the elementary volume (Fig. 2.a). The unknowns $A_{XN}$, $A_{XS}$ and $A_{XP}$ represent respectively the magnetic vector potential at nodes N, S and P.

However, the finite volume discretization scheme represented in (Figure.2.a.) of the elementary volume don´t not take correctly into account the partial derivatives of two different coordinates successively, i.e. the partial differential terms such as:

(9) $$\iiint_{ve}\frac{\partial}{\partial i}(\upsilon\frac{\partial A_k}{\partial j})dv$$

with i≠j and i, j, kare related to the Cartesian coordinates x, y and z. In the new scheme of the elementary volume presented in Fig. 2. b, the terms are described as follows:

(10)
$$\frac{\partial}{\partial y}(\upsilon\frac{\partial A_y}{\partial x})dxdydz = \int_{wb}^{et}\!\!\int(\upsilon\frac{\partial A_y}{\partial x})\Big|_s^n dxdz = \int_{wb}^{et}\!\!\int\left[(\upsilon\frac{\partial A_y}{\partial x})\Big|_n - (\upsilon\frac{\partial A_y}{\partial x})\Big|_s\right]dxdz$$
$$\frac{\partial}{\partial y}(\upsilon\frac{\partial A_y}{\partial x})dxdydz = \left[(\upsilon\frac{\partial A_y}{\partial x})\Big|_n - (\upsilon\frac{\partial A_y}{\partial x})\Big|_s\right]\Delta x\Delta z =$$
$$\left[\upsilon_n\frac{(A_{Yne}-A_{Ynw})}{\Delta xn} - \upsilon_s\frac{A_{Yse}-A_{Ysw}}{\Delta xs})\right]\Delta x\Delta z$$
$$\frac{\partial}{\partial y}(\upsilon\frac{\partial A_y}{\partial x})dxdydz =$$
$$\left[\upsilon_n\frac{(A_{YN}+A_{YP}+A_{YE}+A_{YNE})-(A_{YN}+A_{YP}+A_{YW}+A_{YNW})}{4\Delta xn}\right]\Delta x\Delta z$$
$$-\left[\upsilon_s\frac{(A_{YS}+A_{YP}+A_{YE}+A_{YSE})-(A_{YS}+A_{YP}+A_{YW}+A_{YSW})}{4\Delta xs}\right]\Delta x\Delta z$$
$$\frac{\partial}{\partial y}(\upsilon\frac{\partial A_y}{\partial x})dxdydz =$$
$$\left[\upsilon_n\frac{(A_{YE}+A_{YNE})-(A_{YW}+A_{YNW})}{4\Delta xn} - \upsilon_s\frac{(A_{YE}+A_{YSE})-(A_{YW}+A_{YSW})}{4\Delta xs}\right]\Delta x\Delta z$$

In the new finite volume discretization scheme, it appears supplementary terms such as: $A_{YNE}$, $A_{YNW}$, $A_{YSE}$ and $A_{YNW}$ are defined as a supplementary terms represented in Fig. 2. b for the elementary finite volume (formula 10).

The addition of supplementary nodes to the classical (or basic) elementary volume scheme allows to take into account the successively different partial differential operations applied to different variables (in case of second order partial differential equations). Which leads to a well-treated three-dimensional electromagnetic model, described in equation (10).

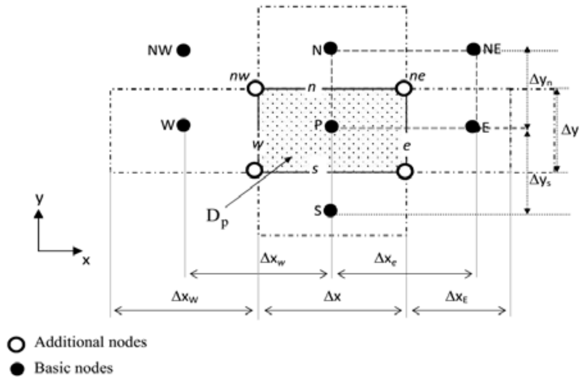


Fig. 3. Projection of the elementary volume according to the XY plane.

**Numerical Results and discussion**

From FVM calculation, both module and the phase of the detected voltage are obtained. From these results, it's possible to determine the impedance. The multilayer characteristics of the specimen (bulk layer + decarburized layer)is taken into account. The mutli-scale time signal (50 Hz-150 kHz) and size (ratio 105 ) are solved.

This multi-scale difference requires adapted meshes depending on the area of sample-sensor system, and a finer time discretization to identify the high-frequency phenomena.

Both figures 4 and 5 represent the comparison between calculated and measured impedance for frequency range values from 50Hz to 150 kHz) and for both specimen surface decarburized layer thickness of L = 200µm and L = 800µm.

According to the presented validation results, it can be concluded that model is robust and can correctly reproduce the impedance profiles for various frequencies. Discrepancies between numerical and experimental results appear for a specimen of L=200µm.

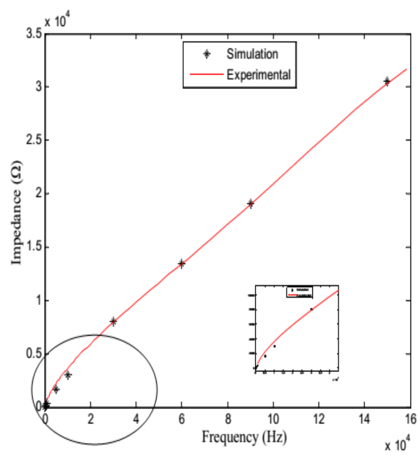


Fig. 4. Calculated and measured impedance profile via frequencies (f = 50Hz-150 kHz) for a specimen with decarburized layer thicknesses L = 800 µm.

Even if these discrepancies are negligible, the FVM presents this limit for applications requiring a fine mesh density. The figure 6 represents the variation of the impedance profile in case of specimen thicknesses: L = 200 µm, 400 µm and 800 µm.
The Figure 7 denotes the impedance for both specimen with decarburized layer thicknesses from 200µm to 800µm. The results show an increase in impedance (an almost linear increase). The Figure 8 represents the two-dimensional distribution of the magnetic field isolines and the value of the magnetic induction for following frequencies f= 50Hz, 1kHz and 150 kHz.

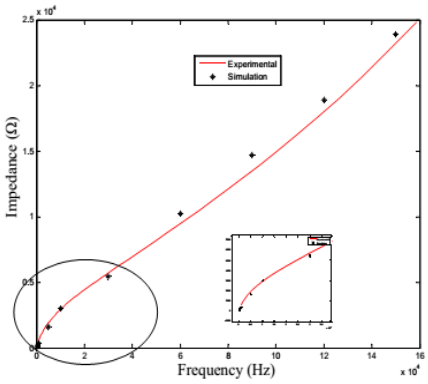


Fig. 5. Computed and measured impedance profile via frequencies (f = 50Hz-150 kHz) for a specimen with decarburized layer thicknesses L = 200 µm.

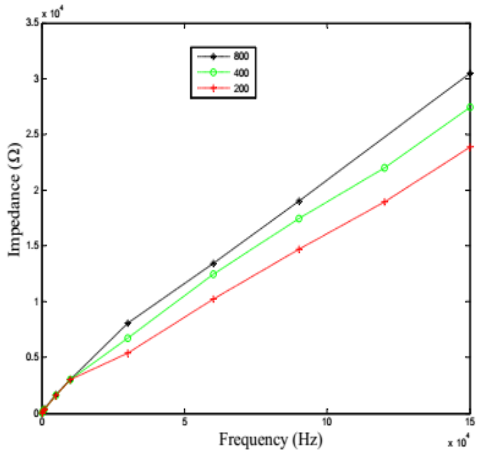


Fig. 6. Calculated impedance profile via frequencies(f = 50Hz-150 kHz) for a specimen with decarburized layer thicknesses L = 800 µm, L = 400 µm and L = 200 µm.

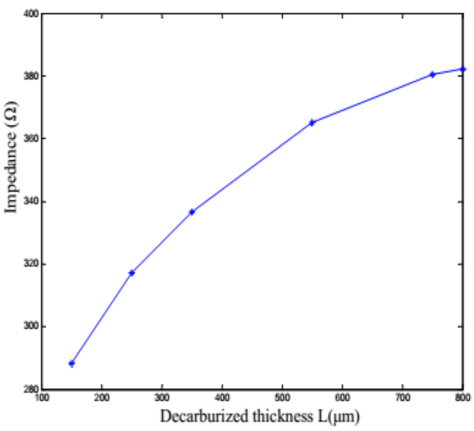


Fig. 7. Impedance values calculated at 1 kHz frequency for various decarburized layer thicknesses L = [150-800]µm.

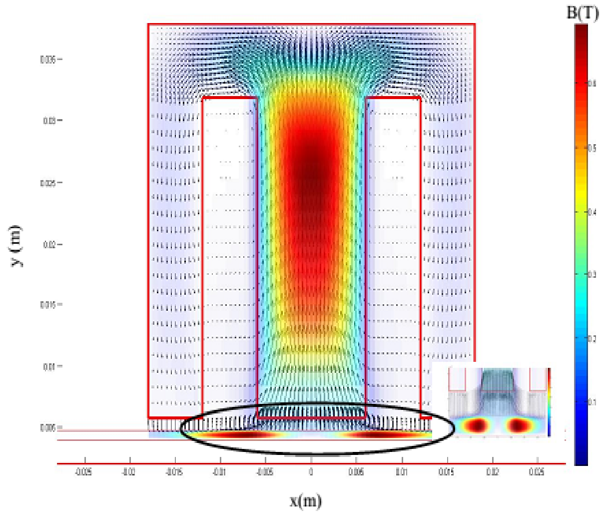


Fig. 8.a. 2D. Distribution of the magnetic field vectors and magnetic induction values for f= 50Hz.

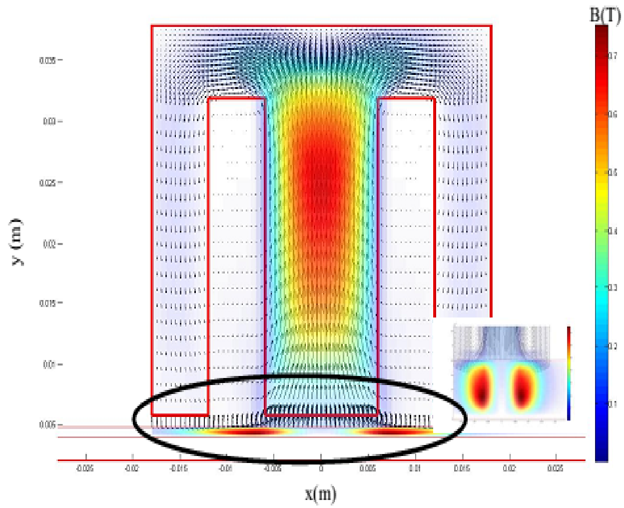


Fig. 8.b. 2D distribution of magnetic field vectors and magnetic induction for f= 1 kHz.

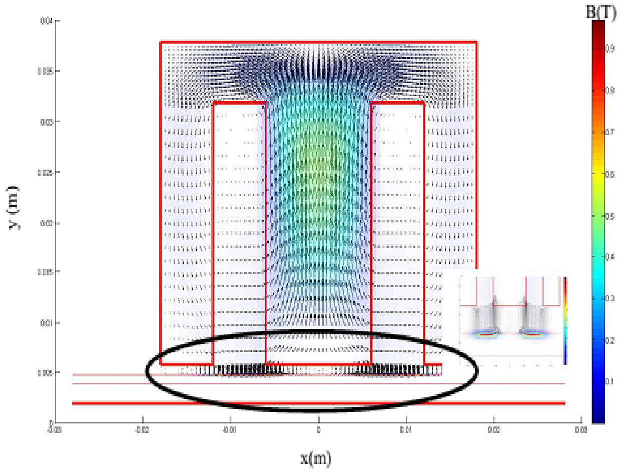


Fig. 8.c. 2D distribution of magnetic field vectors and magnetic induction for f= 150kHz.

## Conclusion

A three-dimensional calculation code implemented under MATLAB environment. In this work, new development were performed and adopt a new approach of the FVM, which makes the analysis of electromagnetic 3D problems possible without simplifying hypothesis. The three dimensional (3D) equation is solved by considering the successively partial derivatives of different coordinates, in case of second order partial differential equation, don't vanishes and included in the final transient algebraic system through the new scheme of finite volume discretization. The comparison between numerical and experimental results show a good agreement results and accuracy. Then, the proposed mathematical of the 3D electromagnetic equation and the associated new finite volume scheme applied. The presented approach limits the FVM for problem, which request very fine meshes.

*Authors: prof. Lotfi Alloui, Laboratoire de Modélisation des Systèmes Energétiques – LMSE; Département d'Electrotechnique, Université Mohamed Kheider, 07000 Biskra, Algeria. E-mail: l.alloui@univ-biskra.dz*

REFERENCES

[1] Y. Gabi, K. Jacob, B. Wolter, C. Conrad, B. Strass, J. Grimm,"Analysis of Incremental and Differential Permeability in NDT via 3DSimulation and Experiment," Journal of Magnetism and Magnetic Materials. vol.505, pp. 339-386, 2020.
[2] V. Hauk, P. Stuitje, Schneider, Eckhardt, and W. A. Theiner, "Comparison of different methods to determine residual stresses nondestructively" in Höller, P. (Hrsg.): New procedures in nondestructive testing. Berlin, Heidelberg, New York: Springer, 1983, S. 561-574.
[3] B. Wolter, C. Boller, C. Conrad, H. G. Herrmann, R. Kern and H. Kopp, "Future trends in steel development, processing technologies and applications" bringing the automotive, supplier and steel industries together. Düsseldorf, (2014) 698-70.
[4] J. Zou, J. S. Yuan, X. S. Ma, X. Cui, S.M. Chen, J. L. He," Magnetic Field Analysis of Iron-Core Reactor Coils by the Finite-VolumeMethod", IEEE Transactions on Magnetics, vol. 40, n° 2, pp. 814-817, 2004.
[5] Y. Gabi," FEM Modelling of a 3MA Non-Destructive Testing System in the Production Line of Dual-Phase Steel," PhD Thesis, 2012, Grenoble, France.
[6] Y. Gabi, D. Böttger, B. Straß, B. Wolter, C. Conrad, F. Leinenbach," LocalElectromagnetic Investigations on Electrical Steel FeSi 3% via 3MA MicromagneticNDT System," 12th European Conference on Nondestructive Testing (ECNDT),Sweden, pp. 11–15, 2018.
[7] C. Amrane, and all,. ' Impact of Lift-Off in 3MA-NDT Harmonic Analysis Signal-via Numerical Methods and Experiment.', December 2021, Przeglad Elektrotechniczny 1(12):47-52
[8] A.Tüysüz, T. Stolz; A. Muetze; M. Flankl; S. Mirić; J. W. Kola," Three-Dimensional Analytical Modeling of an Eddy-Current-Based Non-Contact Speed Sensor", IEEE Open Journal of Industry Applications, vol. 2,pp. 224-234, 2021.
[9] M. Kuczmann, " Overview of the Finite Element Method", ActaTechnica Jaurinensis, vol.8, n°4, pp. 347–383, 2015.
[10] L. Alloui, F. Bouillault, L. Bernard, J. Lévêque, S.M. Mimoune , " 3D Modeling of Forces Between Magnet and HTS in a Levitation System Using New Approach of the Control Volume Method Based on an Unstructured Grid, " Physica C: Superconductivity, vol. 475, pp. 32-37, 2012.
[11] A. Kameni, D. Netter, F. Sirois, B. Douine, J. Lévêque, " New Hybrid FE-FV Method for Computing Current Distribution in 2-D Superconductors: Application to an HTS Cylinder in Transverse Magnetic Field," IEEE Transactions on Applications Superconductors, vol. 19, n°3, 2423 - 2427, 2009.
[12] V. Shankar, W. Hall, H. Mohammadian," A CFD-Based Finite-Volume Procedure for Computational Electromagnet
[13] L. F. Fezoui and S. Lanteri, " Finite Volume Scheme for the 1D Maxwell Equations With GSTC Conditions", [Research Report] RR-9156, Inria, pp.1-14, 2018. ics-Interdisciplinary Applications of CFD Methods," AIAA, pp. 551-564, 1989.
[14] L. Jiangfei and all, "Comparison of Finite Difference and Finite Volume Method for Numerical Simulation of Driven Cavity Flow Based on MAC," 2013 International Conference on Computational and Information Sciences, Lieu ....2013, pp. 891-894.
[15] F. Hermeline and all, "A Finite Volume Method for the Approximation of Maxwell's Equations in Two Space Dimensions on Arbitrary Meshes",Journal of Computational Physics, vol. 227, n° 22, pp 9365–9388, 2008.
[16] L. Alloui and all, "Numerical Study of the Influence of flux Creep and of Thermal Effect on Dynamic Behaviour of Magnetic Levitation Systems With a High-Tc Superconductor Using Control Volume Method", EPJ. App. Phys., vol. 37, n°. 2, pp. 191-195, 2009.
[17] A. Kameni, M. Boubekeur, L. Alloui, F. Bouillault, J. Lambretchs, C. Geuzaine,"A 3-D Semi-Implicit Method for Computing the Current Density in Bulk Superconductors", IEEE Transactions on Magnetics, vol. 50, n°2, pp. 377-380, 2014.